Since January 2020 Elsevier has created a COVID-19 resource centre with free information in English and Mandarin on the novel coronavirus COVID-19. The COVID-19 resource centre is hosted on Elsevier Connect, the company's public news and information website.

Free Radical Biology & Medicine, Vol. 32, No. 7, pp. 584–595, 2002

0891-5849/02/$–see front matter

PII S0891-5849(01)00827-9

Original Contribution

EXTRACELLULAR CYSTEINES DEFINE ECTOPEPTIDASE (APN, CD13) EXPRESSION AND FUNCTION

BEATE FIRLA,* MARCO ARNDT,† KARIN FRANK,† UTE THIEL,† SIEGFRIED ANSORGE,† MICHAEL TÄGER,* and UWE LENDECKEL†

*Institute of Immunology, †Institute of Experimental Internal Medicine, Center of Internal Medicine, Otto-von-Guericke-University of Magdeburg, Magdeburg, Germany

(*Received* 13 *June* 2001; *Accepted* 18 *December* 2001)

Abstract—Alanyl aminopeptidase (APN) is a surface-bound metallopeptidase that processes the N-terminals of biologically active peptides such as enkephalins, angiotensins, neurokinins, and cytokines. It exerts profound activity on vital processes such as immune response, cellular growth, and blood pressure control. Inhibition of either APN gene expression or its enzymatic activity severely affects leukocyte growth and function. We show here that oxidoreductase-mediated modulations of the cell surface thiol status affect the enzymatic activity of APN. Additional evidence for the pivotal role of extracellular cysteines in the APN molecule was obtained when substitution of any of these six cysteines caused complete loss of surface expression and enzymatic activity. In contrast, the transmembrane Cys24 appears to have no similar function. Enzymatically inactive cysteine mutants were retained in the endoplasmic reticulum as shown by high-resolution imaging and Endoglycosidase H digestion. In the absence of any crystal-structure data, the demonstration that individual extracellular cysteines contribute to APN expression and function appears to be of particular importance. The data are the first to show thiol-dependent modulation of the activity of a typical surface-bound peptidase at the cell surface, probably reflecting a general regulating mechanism. This may relate to various disease processes such as inflammation or malignant transformation. © 2002 Elsevier Science Inc.

Keywords—Aminopeptidase N, Proteindisulfide isomerase, Thiol status, Disulfide bond, Site-directed mutagenesis, Free radicals

INTRODUCTION

Human alanyl aminopeptidase (aminopeptidase N, APN, CD13; EC 3.4.11.2) is a 150 kDa metalloprotease (M1 family, clan MA, gluzincins) [1,2] that shows preferential cleavage of neutral amino acids from the N-terminus of oligopeptides. This type II membrane protein with its zinc-dependent catalytic activity is constitutively expressed on the surface of a wide variety of cells and it has been identified as the leukocyte surface differentiation antigen CD13 [3]. The human APN gene, the coding sequence of which is spread over 20 exons [4], was cloned and mapped to chromosome 15 (*q25–q26*) [5,6].

Alanyl aminopeptidase is expressed greatly in the small intestine where it participates in the final hydrolysis of ingested nutrients. It is also expressed in the kidney and to a lesser extent in other tissues [7,8]. However, the physiological role of alanyl aminopeptidase on the surface of immune cells has not been fully established. It is believed to be involved in the degradation of neuropeptides [9–11] and cytokines [12,13], and, furthermore, it may well contribute to matrix degradation, angiogenesis, and antigen processing [14–17]. Alanyl aminopeptidase also functions as a receptor for corona viruses [18,19] and CMV [20].

With respect to the hematopoietic system, APN is predominantly expressed on cells of myelo-monocytic lineage [21]. While mature B cells and resting T cells lack detectable APN expression, acute and chronic B cell leukemia show an abnormal surface expression of alanyl aminopeptidase, which is associated with a poor prognosis in the case of adult B-ALL (acute B cell leukemia) [22,23]. A marked increase in the expression of CD13 is found on the surface of T cells activated by mitogens in

Address correspondence to: Dr. Beate Firla, Institute of Immunology, Otto-von-Guericke-University of Magdeburg, Leipziger Strasse 44, D-39120 Magdeburg, Germany; Tel: +49 391-6714451; Fax: +49 391-6715852; E-Mail: beate.firla@medizin.uni-magdeburg.de.

vitro [24–26] or derived from local sites of inflammation in vivo [27,28]. Furthermore, T lymphocytes show an activation-dependent increase in APN gene expression [29,30]. Antiproliferative effects result from inhibition of both alanyl aminopeptidase activity and expression [30, 31]. This suggests a link between APN expression and leukocyte proliferation as recently reviewed by Lendeckel et al. [32].

The crystal structures of APN or related surface proteases have not yet been resolved. Since a number of these related enzymes share the feature of conserved extracellular cysteine residues, knowledge of the function of these residues may improve the proposed structure models for these enzymes. Cysteine residues are generally of particular importance for formation and maintenance of protein structure and, consequently, function.

To establish the role of cysteine residues in the maintenance of the tertiary structure of a membrane-bound surface protease, modulations of the cell surface thiol status are carried out. Thiols located on the cell surface are mainly represented by proteinogenic cysteinyl groups. On B-CLL cells, the regulation of this surface thiol status is tightly controlled by membrane-bound oxidoreductases, such as proteindisulfide isomerase (PDI), which catalyze sulfhydryl-disulfide interchange reactions at the cell surface [33]. The inhibition of PDI on viable cells leads to a dramatic rise in total surface thiol expression, which is at least partly due to an increase in cysteine-derived SH groups. Furthermore, γ-glutamyl transpeptidase (GGT) is known to be involved in redox modulations of cell surface protein thiols by its participation in the metabolism of glutathione [34]. Similar to PDI inhibition, inhibition of γ-glutamyl transpeptidase leads to an increased amount of surface thiols. Therefore, modulations in the surface thiol status of U937 cells are carried out by inhibiting PDI by bacitracin and inhibitory antibodies or by inhibiting GGT by acivicin.

To evaluate the role of each individual cysteine in the APN, site-directed mutagenesis was applied. As deduced from its coding sequence [35], human alanyl aminopeptidase, a 967-amino acid protein, contains seven cysteine residues at positions 24, 113, 223, 761, 768, 798, and 834, which are all highly conserved between APNs from different species [36]. The first cysteine is located in the transmembrane region of the enzyme, while the latter six cysteines are located in the extracellular part, which also contains the active site with the HEXXH motif (amino acids 388 to 392). In earlier studies, it was shown that correct folding of the extracellular part of APN occurs independently of the residual protein [37], which suggests that substitution of cysteine 24 will not affect structure and function of alanyl aminopeptidase. In contrast, the effects of substituting cysteine residues in the extracellular part are not as predictable since alanyl aminopeptidase is known to be expressed as a homodimer of two noncovalently linked subunits [38]. However, it does seem reasonable to suppose that disulfide bridges are involved in the formation of the tertiary structure of alanyl aminopeptidase, especially within its C-terminal domain [39].

Our data indicate that (i) oxidoreductase-mediated modulations of the cell surface thiol status significantly affect the enzymatic activity of APN and (ii) the substitution of distinct cysteine residues in the extracellular portion of alanyl aminopeptidase leads to an ER retardation of enzymatically inactive mutant proteins. These findings suggest that all extracellular cysteine residues are involved in the correct formation of the tertiary structure of alanyl aminopeptidase and they support the concept that intramolecular disulfide bridges are formed within the extracellular part of APN. Moreover, these results may imply a general regulatory mechanism for ectopeptidase activity at the cell surface that is based on thio-disulfide interchange reactions.

MATERIALS AND METHODS

Materials

CombiPol DNA Polymerase Mix was obtained from Invitek (Berlin, Germany); DNA oligonucleotides (purified by reversed-phase chromatography, 5′-phosphorylated for site-directed mutagenesis) were from BioTez Berlin-Buch GmbH (Berlin, Germany); T4 DNA ligase, all restriction enzymes, Endo H_f, and PNGase F were from New England Biolabs (Beverly, MA, USA); and Transfection reagent Effectene was from QIAGEN (Santa Clarita, CA, USA). The fluorescent probes ER-Tracker Blue-White DPX and BODIPY TR ceramide were purchased from Molecular Probes (Eugene, OR, USA). Cells were routinely grown at 37°C, 5% CO_2, and 94% humidity. EcR-293 cells were obtained from Invitrogen (Groningen, The Netherlands) and grown in DMEM with 10% FCS (Gibco BRL, Grand Island, NY, USA) and 400 μg/ml Zeocin (Invitrogen). U937 cells (ATCC) were cultured in RPMI 1640 (Gibco BRL)/10% FCS.

Modulations of the cell surface thiol status

For inhibition of PDI, U937 cells were cultured in the presence of bacitracin (Sigma Chemical Co., St. Louis, MO, USA) or anti-PDI mAb clone C1D11 [33], both of which specifically inhibit the oxidoreductase activity of PDI. Cultures without bacitracin and with murine IgG (Sigma Chemical Co.) served as controls. Furthermore, U937 cells were cultured in the presence of different

Table 1. Mutagenic Oligonucleotides for Site-Directed Mutagenesis of APN

Name	Sequence			
C24G-s	5′-GGCGTGGCAG	CCGTG**g**GCAC	AATCATCGCA	CTGTCA
C24G-as	5′-TGACAGTGCG	ATGATTGTGC	**c**CACGGCTGC	CACGCC
C113F-s	5′-ACCGTCCGTT	TCACCT**tt**AA	AGAGGCCACT	GACGTC
C113F-as	5′-GACGTCAGTG	GCCTCTTT**aa**	AGGTGAAACG	GACGGT
C223W-s	5′-CGGAAGTCCT	TCCCATG**g**TT	CGATGAGCCG	GCC
C223W-as	5′-GGCCGGCTCA	TCGAA**c**CATG	GGAAGGACTT	CCG
C761G-s	5′-GCCATCAGCA	CCGCC**g**GCTC	CAACGGAGTT	CCA
C761G-as	5′-TGGAACTCCG	TTGGAGC**c**GG	CGGTGCTGAT	GGC
C768G-s	5′-AACGGAGTTC	CAGAG**g**GTGA	GGAGATGGTC	TCT
C768G-as	5′-AGAGACCATC	TCCTCAC**c**CT	CTGGAACTCC	GTT
C798W-s	5′-CGGTCCACCG	TCTACTG**g**AA	CGCTATCGCC	CAG
C798W-as	5′-CTGGGCGATA	GCGTT**c**CAGT	AGACGGTGGA	CCG
C834G-s	5′-CGGGCAGCCC	TGGCC**g**GCAG	CAAAGAGTTG	TGGATC
C834G-as	5′-GATCCACAAC	TCTTTGCTGC	**c**GGCCAGGGC	TGCCCG

Mismatches with the template are indicated by bold lowercase letters.

thiol effectors or in thiol-deficient medium for the indicated periods of time. The following were used as thiol effectors: acivicin (Sigma Chemical Co.), inhibiting GGT; BSO (Sigma Chemical Co.), inhibiting γ-glutamylcysteine synthetase; NEM or diamide.

Washed samples were analyzed as follows: flow cytometrically to assess APN immunoreactivity to the anti-APN mAbs clone WM15 and Leu-M7 and for their Ala-pNA (alanylparanitroanilide) hydrolyzing activity [40].

Construction of a wild-type APN-GFP fusion protein

APN cDNA was amplified by PCR from U937 cDNA using following primers: primer 1, d(AGC CGG CTA GCC ACC ATC ACC ATG GCC AAG GGC); primer 2, d(GAT CCG CGG TTT GCT GTT TTC TGT GAA). The fragment was cloned into pEGFP- N1 vector (Clontech, Palo Alto, CA, USA), which resulted in the expression vector (pEGFP-APN) containing enhanced GFP (green fluorescent protein) in frame to the 3′ end of wild-type APN.

Construction of mutant APN-related GFP fusion proteins

Different mutations were introduced into pEGFP-APN by site-directed mutagenesis using QuickChange site-directed mutagenesis kit (Stratagene, La Jolla, CA, USA). Amplification of the original vector using *Pfu* polymerase and mutagenic oligonucleotides (see Table 1) was carried out. Afterwards the parental vector was digested by restriction enzyme *Dpn* I. The nicked vector was transformed into *E. coli* TOP 10 (Invitrogen). Two preparations of each vector were obtained: pEGFP-APN-C24G, -C113F, -C223W, -C761G, -C768G, -C798W, and -C834G.

The double mutant C24G/C834G was constructed using the vector pEGFP-APN-C24G as a template, yielding the expression vector pEGFP-APN-C24G/C834G. The resulting constructs containing the different mutations were analyzed by restriction analysis, immunoblotting, and fluorescence of the expressed mutant GFP fusion proteins.

Transfection of EcR-293 cells

The constructed vectors were transiently transfected into EcR-293 cells using the Effectene transfection reagent (QIAGEN). In 6-well format, 3×10^5 cells per well were seeded the day prior to transfection. For complex formation, 0.4 μg DNA, 3.2 μl Enhancer, and 5 μl reagent were used. Cells were cultured for 2 d before assayed.

Fluorescence microscopy

Transfected cells grown on glass coverslips were analyzed using an Axiovert 135 TV (Zeiss, Göttingen, Germany) equipped with the Spot RT Slider camera, and Meta Series and Auto Deblur software (Visitron Systems, Puchheim, Germany) at 100× magnification. GFP fluorescence was detected using the filter set 10 (Zeiss).

Colocalization studies with organelle-specific fluorescent probes were performed. Cells grown on coverslips for 2 d were washed once with HBSS/10 mM HEPES. To stain the ER, cells were incubated with 200 nM ER-Tracker Blue White DPX in HBSS/10 mM HEPES for 30 min at 37°C and washed once with PBS. Blue fluorescence was detected using filter set 01 (Zeiss). To stain the Golgi, cells were incubated with 5 μM BODIPY TR ceramide-BSA-complex in HBSS/10 mM HEPES for 10 min at 37°C and washed once with PBS. Red fluorescence was detected using filter set 00 (Zeiss).

Cytofluorimetric analyses

Surface staining of cells was performed at 4°C for 30 min using anti-CD13 (clone WM15, Pharmingen [Heidelburg, Germany] and WM15 PE-conjugate, Dianova [Hamburg, Germany]; clone Leu-M7, PE-conjugate, Becton Dickinson [Mountain View, CA, USA]); and anti-GFP antibodies (Living Colors Peptide antibody, Clontech). After two washes in cold PBS, cells were incubated with goat-antimouse PE-conjugate (Dianova) for WM15 staining or donkey-antirabbit PE-conjugate (Dianova) for anti-GFP staining, both at 4°C for 30 min. Cells were washed twice in cold PBS prior to analysis. For staining of cytoplasmic epitopes, permeabilization of cells was performed with a cell permeabilization kit (Fix & Perm, An der Grub Bio Research GmbH, Kaumberg, Austria) before staining. Cytofluorimetric analysis was performed using FACS Calibur (Becton Dickinson) on readings from 5000 cells per sample. Data are given as mean fluorescence intensities (mfi) ± SEM.

Preparation of the particulate fraction

Cells (2×10^6) were resuspended in PBS and lyzed by sonication on ice for 30 min. The suspension was centrifuged at 60,000 × *g* for 30 min and then resuspended in either 500 μl PBS (for activity measurements) or 100 μl denaturing buffer (New England Biolabs) containing 1% β-mercaptoethanol and 0.5% SDS (for digestion and blotting analyses) using sonication.

Digestion with Endo H_f and PNGase F

The particulate fraction was boiled for 10 min. For Endo H_f digestion, 10 μl of the particulate fraction were incubated with 1 μl 10 × G5 buffer and 2000 U Endo H_f for 1 h at 37°C. The particulate fraction treated the same way, except for the addition of Endo H_f, served as a control. PNGase F digestion was carried out in 10 μl of the particulate fraction using 1 μl 10 × G7 buffer, 1 μl NP40 (10%), and 500 U PNGase F for 1 h at 37°C.

Immunoblotting

The particulate fractions resuspended in denaturing buffer were supplemented with two volumes Laemmli buffer (Bio-Rad, Hercules, CA, USA) and boiled for 2 min. Probes were separated on 4–12% gradient NuPage gels using MOPS-SDS running buffer (Invitrogen) at 15°C. Two different protein markers, SeeBluePlus2 Prestained Standards (Novex) and Prestained Precision Protein Standards broad range (Bio-Rad), were used to estimate protein size. After blotting on to a Protran BA-85 membrane (Schleicher & Schüll, Keene, NH, USA), APN-GFP fusion proteins were detected by means of Living Colors Peptide antibody (Clontech), goat-antirabbit-HRP (horseradish peroxidase, New England Biolabs), and SuperSignal West Dura Extended Duration chemoluminescence substrate (Pierce, Bonn, Germany).

Enzymatic assay

The particulate fractions resuspended in PBS were used to determine the enzymatic activity. To normalize the activities, the GFP fluorescence of each probe was measured using a luminescence spectrophotometer LS 50 (Perkin Elmer, Norwalk, CT, USA) with excitation at 488 nm and emission at 507 nm. Neutral aminopeptidase activity was determined by measuring the hydrolysis of Ala-pNA [40]. The specific activity was calculated as follows:

$$a_{specific} = a_{measured} * I_{GFP}\,(nontransfectedcells)/I_{GFP}.$$

RESULTS

Effects of PDI inhibition on the enzymatic activity of surface-bound APN

The myelo-monocytic cell line U937, coexpressing APN and the oxidoreductase PDI at the cell surface, was used to elucidate the influence of oxidoreductase-mediated changes of the cell surface thiol status on APN activity. Treatment of U937 cells with the PDI inhibitor bacitracin resulted in a concentration- and time-dependent increase in their immunoreactivity to the anti-APN clone Leu-M7 (Table 2). In contrast, the immunoreactivity of the anti-APN clone WM15 was found to be significantly decreased. After 48 h, and more pronounced after 72 h, the addition of 100 μM bacitracin led to a 1.6-fold decrease in WM15 reactivity compared to the control. In parallel, the Ala-pNA hydrolyzing activity was reduced to 78% after 48 h and to 68% after 72 h (Table 2) in comparison to untreated controls.

The possibility that these changes resulted from effects other than inhibition of oxidoreductase activity was excluded by showing that the anti-PDI mAb clone C1D11, known to inhibit PDI catalytic activity [33], affected APN activity equally. After 48 h in presence of anti-PDI mAbs, a concentration-dependent increase in Leu-M7 immunoreactivity was observed, whereas the WM15 reactivity was significantly decreased. As shown in Fig. 1, the opposite kinetics of the two anti-APN mAb clones became evident at concentrations as low as 0.2 μg/ml anti-PDI mAb C1D11 (mean fluorescence intensities of 573.7 ± 12.4 and 402.3 ± 3.8 for Leu-M7 and WM15, respectively) and enhanced at 2 μg/ml C1D11

Table 2. Immuoreactivity of Anti-APN mAbs and Enzymatic Activity of APN on U937 Cells After Inhibition of PDI by Bacitracin

	After 48 h						After 72 h					
	Leu-M7		WM15		Ala-pNA-hydrolysis		Leu-M7		WM15		Ala-pNA-hydrolysis	
Bacitracin	(mfi)	SEM	(mfi)	SEM	(%)	SEM	(mfi)	SEM	(mfi)	SEM	(%)	SEM
Control	416.0	4.2	416.6	8.7	100.0	–	427.0	6.6	414.0	7.4	100.0	–
10 μM	584.0	7.2	369.0	11.0	91.0	2.9	618.6	11.0	354.7	8.4	83.7	1.4
100 μM	667.0	13.3	288.7	6.1	77.7	2.6	759.7	12.0	254.3	8.1	67.7	4.7

All data are given as mean ± SEM of three experiments.

(mfi of 686.0 ± 3.6 for Leu-M7 and 272.0 ± 5.8 for WM15). Murine IgG, supplemented at concentrations equal to anti-PDI mAb, failed to show any effect on APN immunoreactivity.

Effects of other thiol effectors on the enzymatic activity of surface-bound APN

To compare the observed effects of the PDI inhibition at the surface of U937 cells with effects caused by other thiol effectors, U937 cells were cultured in the presence of 150 μM acivicin, 500 μM BSO, 100 μM NEM, or 50 μM diamide (Table 3). In contrast to PDI inhibition, these thiol effectors did not cause significant alterations of the immunoreactivity against both anti-APN mAb clones. The diminished reactivity against both mAb clones after BSO treatment may represent a decreased amount of APN-molecules at the cell surface.

Cellular and functional characteristics of the APN-GFP fusion protein

To determine the subcellular localization of wild-type and mutated alanyl aminopeptidase proteins, fusion proteins, with enhanced GFP (EGFP) fused in frame to the C-terminus of APN, were constructed. The C-terminal attachment of GFP to wild-type APN did not change either its subcellular localization or its function: the typical surface expression of wild-type alanyl aminopeptidase was completely retained (Fig. 2A). This implies that protein folding, glycosylation pattern, and intracellular transport were not markedly influenced. Results of cytofluorimetric analyses confirmed the intense surface expression of APN-GFP when using either anti-GFP or anti-CD13 antibodies. The mean fluorescence intensities were increased significantly when compared with nontransfected cells (Table 4). Furthermore, the neutral aminopeptidase activity of the wild-type enzyme was fully preserved. The Ala-pNA hydrolyzing activity of the particulate fraction of EcR-293 cells was significantly increased upon transient transfection with pEGFP-APN in comparison to nontransfected cells that showed only 47.7% of wild-type activity (Fig. 3, black columns). Further evidence for the structural integrity of the wild-type APN-GFP fusion protein was obtained from SDS-PAGE and immunoblot analysis of the particulate fraction of EcR-293 cells. Using an anti-GFP antibody, two bands of approximately 170 and 190 kDa were detected. The band with the higher molecular weight corresponds to the 166 kDa monomeric form of mature APN enlarged by 27 kDa of monomeric GFP (Fig. 4, lane 2). The double band that was detected represents different glycosylation forms, as confirmed by PNGase F treatment, which leads to a single band of approximately 140 kDa. Endoglycosidase H digestion resulted in degradation of the lower molecular weight species, indicating that this was a mannose-rich glycosylation form of APN (Fig. 5).

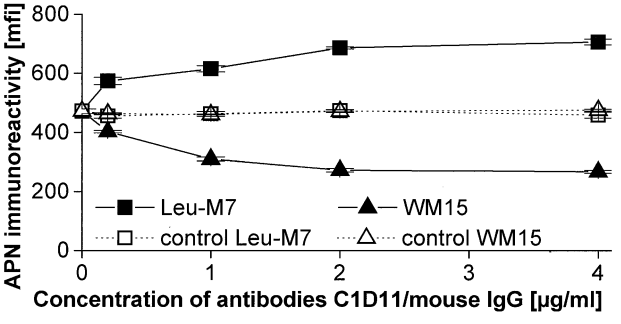

Fig. 1. Influence of anti-PDI mAbs on the cell surface immunoreactivity of APN. U937 cells were cultured in presence of anti-PDI clone C1D11 (filled lines) or mouse IgG (pointed lines, control). After 48 h, the immunoreactivity of anti-APN mAbs, clone Leu-M7 (■) and clone WM15 (▲), at the cell surface was determined by flow cytometry. Data are given as mean ± SEM of mfi; $n = 3$.

Integrity of the mutant proteins

To examine the integrity of the mutants, APN-GFP fusion proteins were expressed in EcR-293 cells and analyzed for GFP-fluorescence by means of fluorescence microscopy. Protein size was determined by using reduc-

Table 3. Immuoreactivity of Anti-APN mAbs on U937 Cells After Modulation of the Thiol Status

Effector	Concentration (μM)	Time (h)	n	Leu-M7 Ratio	Leu-M7 SEM	WM15 Ratio	WM15 SEM
Acivicin	150	1	3	1.02	0.04	1.06	0.13
Acivicin	150	4	4	0.92	0.10	0.94	0.41
BSO	500	4	4	0.92	0.14	0.71	0.11
NEM	100	1	4	0.86	0.22	1.10	0.31
Diamide	50	1	4	0.96	0.04	0.88	0.09

All data are given as a mean ratio between mfi values for effector-treated and untreated cells ± SEM.

ing SDS-PAGE followed by Western blotting and detection with an anti-GFP antibody.

All constructs yielded intense GFP fluorescence upon transfection into EcR-293 cells. Furthermore, all mutant proteins showed immunoreactivity to an anti-GFP-Ab. Compared to the wild-type APN-GFP, no apparent alterations in the electrophoretic mobility in SDS-PAGE were detected for the C24G mutant. In contrast, all other mutants showed a single band only, which probably corresponded to the Endoglycosidase H-sensitive form of the wild-type protein (Fig. 4). These findings indicate that the primary structure of the protein was not severely impaired. In contrast, the glycosylation pattern seemed to be affected by substitution of extracellular cysteine residues.

The expression levels of the individual APN-GFP fusion proteins showed significant variations (Fig. 4). To compensate for these differences, which were due to variations in the transfection efficiency and expression levels, the intensity of GFP-specific fluorescence was used to normalize the enzymatic activity data.

Enzymatic activity of mutant alanyl aminopeptidase

EcR-293 cells, transiently transfected with mutant APN-GFP, were analyzed for neutral aminopeptidase activity (Fig. 3). It was confirmed that all mutants showed high levels of GFP fluorescence as well as immunoreactivity to an anti-GFP-mab, indicating a proper folding of the GFP chromophore. Therefore, GFP fluo-

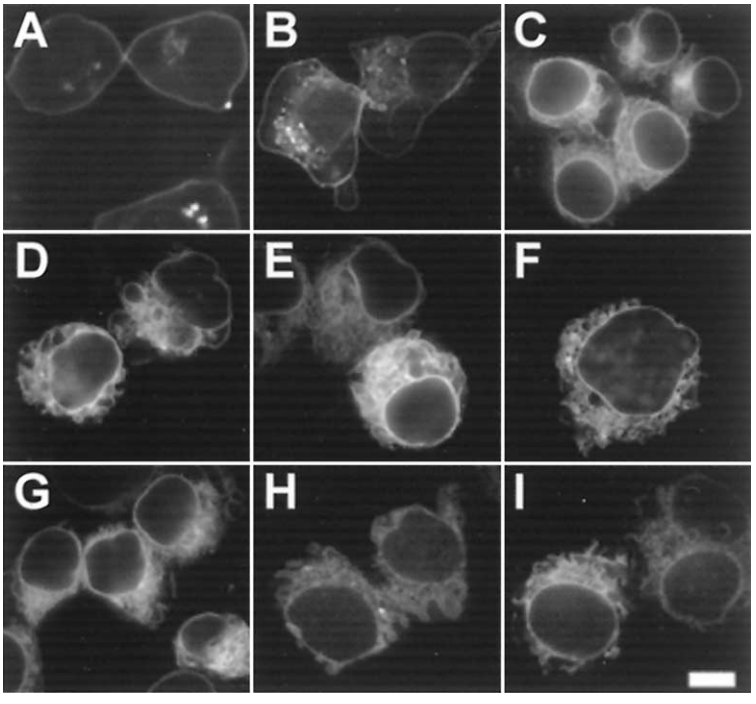

Fig. 2. Fluorescence microscopy of EcR-293 cells expressing different APN-GFP fusion proteins. Images were collected with Axiovert 135 TV (Zeiss) fitted with fluorescein filters at 100× magnification applying exposure times between 0.5 and 2.0 s. (A) Expression of wild-type APN-GFP fusion protein; (B)–(I) expression of APN-GFP fusion proteins with the following mutations: (B) C24G; (C) C113F; (D) C223W; (E) C761G; (F) C768G; (G) C798W; (H) C834G; (I) C24/834G; bar = 10 μm.

Table 4. Cytofluorimetric Analyses of APN-GFP Fusion Proteins

	Leu-M7 (%)	WM15 (%)
Control	0.0	0.0
Wild-type	100.0	100.0
C24G	87.6	86.1
C113F	15.5	2.3
C223W	17.3	1.3
C761G	2.2	1.9
C768G	11.1	3.4
C798W	1.9	2.1
C834G	3.4	2.1
C24/834G	2.9	2.2

Data given as relative mean fluorescence intensities; staining with mAbs after permeabilization of the cells.

rescences were used to normalize the enzymatic activities as described in Materials and Methods in detail. Each mutant was represented by two independent plasmid clones (striped and white columns). As expected, the mutation C24G did not decrease the enzymatic activity of APN. The specific activity of C24G-transfected cells was significantly increased in comparison to nontransfected control cells and it even exceeded that of wild-type APN (148.5 and 154.5% of wild-type activity). In contrast, all other mutants showed a marked decrease in specific activities to less than 42% of wild-type activity in all cases ($p = .052$ and .07 for C223W clones 1 and 2, respectively; $p < .05$ in all other cases), representing a decrease in wild-type activity back to the control level.

Subcellular localization of the mutant proteins

Surface expression of mutant APN-GFP fusion proteins was analyzed by fluorescence microscopy and cytofluorimetric analysis in EcR-293 cells transiently transfected with the appropriate expression vectors. The substitution of cysteine residue 24 had no effect on the surface expression of APN (Fig. 2B). This is in full agreement to the corresponding enzymatic activity, which also was not affected by the substitution of this residue. All others provoked changes in the expression pattern of the APN-GFP fusion proteins, with apparently predominant intracellular localization (Figs. 2C–2I). This was confirmed by cytofluorimetric analysis using an anti-GFP antibody. A clear-cut surface expression was observed only in cells transfected with either wild-type APN-GFP or the C24G mutant (27% positive cells, mfi of 200.2 and 224.1, respectively, compared to less than 4% positive cells and mfi < 45 for all other mutants).

Therefore, detailed colocalization studies were used to investigate the subcellular localization. We used different reference markers for Golgi and ER structures. These studies were performed with all the mutants that did not contain C24G mutation. Mutants containing the C24G substitution were not included since this mutation failed to show any changes in the expression pattern of APN.

For selective staining of ER, ER-Tracker Blue-White DPX was used. The resulting fluorescence showed a typical ER-staining pattern around nonfluorescent cell nuclei (Fig. 6B). Using BODIPY TR ceramide as a trans-Golgi probe, a staining pattern that was evidently different from the ER staining was observed (Fig. 6E). As illustrated in Fig. 6 using the C113F mutant, a clear overlap of the GFP-derived fluorescence with an organelle-specific marker was only observed with the ER staining. Some partial overlap in the case of Golgi staining may have been due to high background fluorescence. Similar results were obtained for the other mutants, indicating that all enzymatically inactive mutants are retained in the ER.

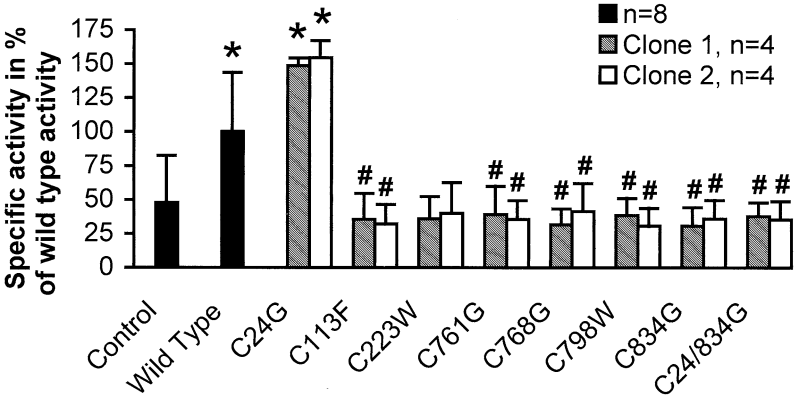

Fig. 3. Neutral aminopeptidase activity of EcR-293 cells expressing different APN-GFP fusion proteins. Specific activities of the particulate fractions of transiently transfected EcR-293 cells were measured. Nontransfected cells served as a control. Every experiment was normalized using the mean of the wild-type APN-GFP fusion protein. Results are given as percentages of wild-type activity (46.6 pkat/10^6 cells). *A significant increase compared with the control; #a significant decrease compared with the wild-type protein (one-way ANOVA, $p < .05$).

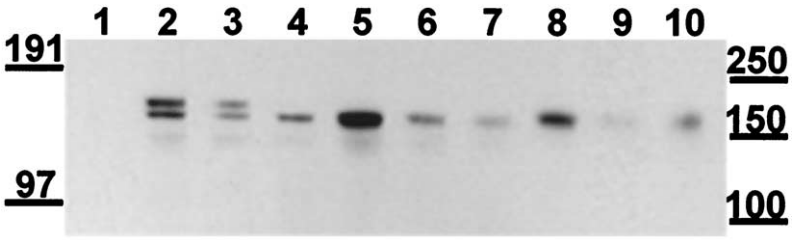

Fig. 4. Expression of different APN-GFP fusion proteins in EcR-293 cells. The particulate fraction of transiently transfected EcR-293 cells was analyzed using reducing SDS-PAGE (4–12%) and immunoblotting. APN-GFP fusion proteins were detected using an anti-GFP antibody. M = bands of two protein markers; 1 = control; 2 = wild-type; 3 = C24G; 4 = C113F; 5 = C223W; 6 = C761G; 7 = C768G; 8 = C798W; 9 = C834G; 10 = C24G/C834G.

To confirm these results, analysis of Endoglycosidase H sensitivity and PNGase F treatment were carried out for all APN-GFP fusion proteins. Treatment with Endo H distinguishes high mannose (sensitive) from complex (insensitive) sugars, and, thus, indicates whether a protein is able to leave the ER. Digestion with PNGase F enables one to determine whether different protein forms are due to variations in the glycosylation pattern.

In all cases, the PNGase F digestion resulted in the formation of one single band of lower molecular weight (Fig. 6). A band of approximately 140 kDa was detected (unglycosylated APN (115 kDa) enlarged by the monomeric GFP). Corresponding to the results for wild-type protein, the double band detected in the case of the C24G mutant was reduced to a single band after PNGase F treatment, which suggests that two different glycosylation forms are present in the particulate fraction.

Treatment with Endo H revealed the presence of Endo H-sensitive proteins in all particulate fractions. One additional insensitive band of higher molecular weight, corresponding to the complex glycosylated mature form of APN that is transported to the cell surface, was found only for the wild-type APN and the C24G mutant. In contrast, in all other cases the GFP fusion protein was completely sensitive to Endo H, confirming the results of the colocalization studies, which showed a clear ER retardation of these proteins.

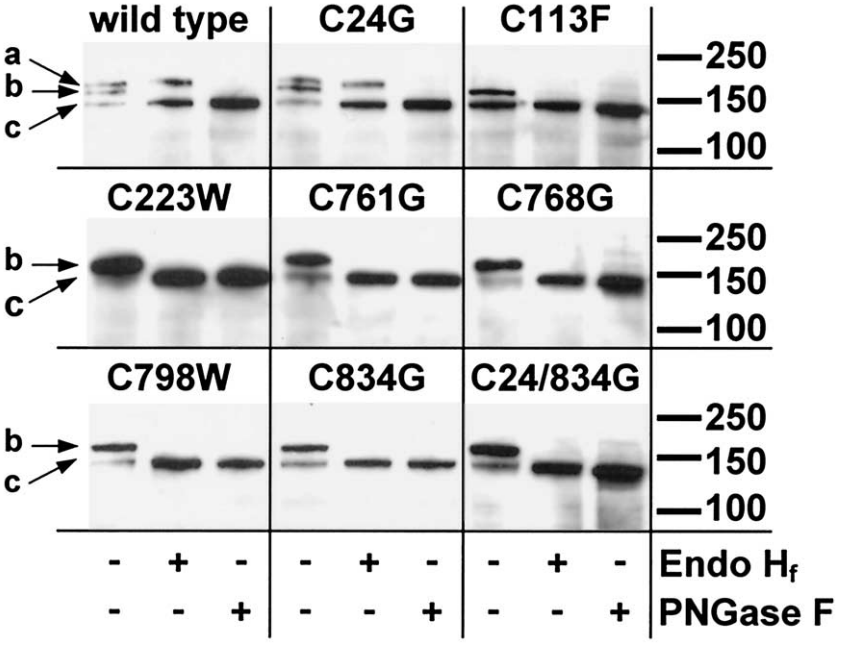

Fig. 5. PNGase F and Endoglycosidase H treatment of APN-GFP fusion proteins. Particulate fractions of EcR-293 cells expressing APN-GFP fusion proteins were incubated with or without PNGase F/Endoglycosidase H as indicated below and separated on 4–12% gradient gels. Bands of the protein marker are indicated on the right. Three protein bands were detected: a = high molecular weight, not Endo H-sensitive; b = medium molecular weight, Endo H-sensitive; c = low molecular weight, deglycosylated form.

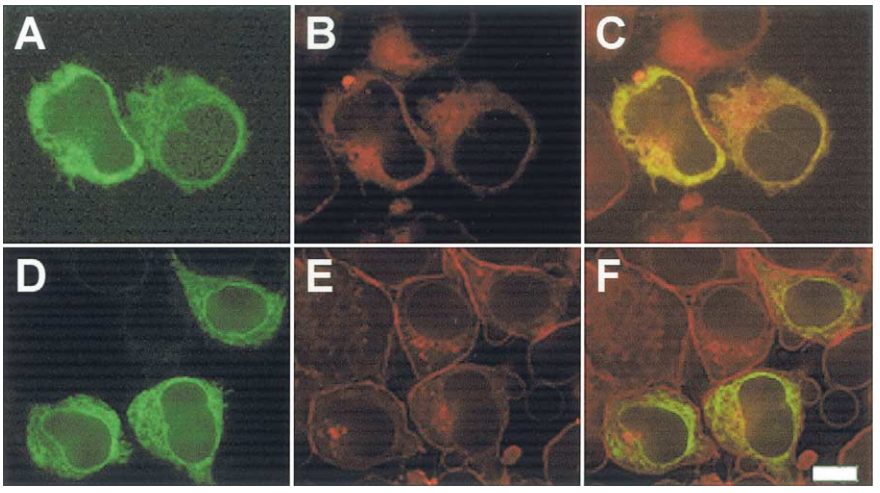

Fig. 6. Colocalization studies of EcR-293 cells expressing mutant APN-GFP fusion protein. Cells were stained with ER-Tracker Blue-White DPX or BODIPY TR ceramide. Colocalization is shown for the C113F mutant. The GFP-derived fluorescence is shown in green and the fluorescence of the ER or Golgi marker is shown in red. (A) GFP signal of C113F; (B) ER staining of the same cells; (C) colocalization of C113F with ER; (D) GFP signal of C113F; (E) Golgi staining of the same cells; (F) colocalization of C113F with Golgi; bar = 10 μm.

Immunoreactivity against anti-CD13 monoclonal antibodies

Cytofluorimetric analysis of permeabilized cells unexpectedly revealed that the substitution of cysteine residues 761, 798, and 834 was obviously associated with a complete loss of the epitope recognized by the anti-CD13 monoclonal antibody clone Leu-M7. Thus, both the single mutants C761G, C798W, C834G, and the double mutant C834G/C24G showed Leu-M7 immunoreactivity of less than 4% of the wild-type mfi, while in all other cases mfi values of more than 10% were retained (Table 4). Notably, none of the enzymatically inactive mutants bound to the anti-CD13 monoclonal antibody clone WM15 (Table 4).

DISCUSSION

Cysteine residues are known to be of particular importance in the formation and maintenance of tertiary protein structures. The aims of the present study were (i) to elucidate the influence of oxidoreductase-mediated modulations of the cell-surface thiol status on the enzymatic activity of APN on the surface of viable cells, and (ii) to use site-directed mutagenesis to study the functional role of each individual cysteine residue of APN on surface expression/subcellular localization, enzymatic activity, and binding to anti-CD13 mAbs.

Utilizing glutathione, proteindisulfide isomerase catalyzes the formation of inter- and intramolecular disulfide bridges [41]. The inhibition of PDI by either bacitracin or inhibitory monoclonal antibodies on the cell surface results in reduced enzymatic activity of APN. Thus, it is evident that the cysteine-linked sulfhydryl-disulfide turnover at the cell surface can modulate APN enzymatic activity. As expected from studies that characterized the anti-APN mAb clone WM15 as being inhibitory [42], the immunoreactivity of this clone was equally diminished. This effect is not due to a loss of APN on the cell surface, since, under the same conditions, the reactivity to the anti-APN mAb clone Leu-M7, which does not affect APN activity, was found to be increased. This could be due to the larger distance of the relevant epitope from the catalytic center, which was concluded from the finding that substitution of cysteine residues 761, 798, and 834 did cause a complete loss of Leu-M7 binding. Thus, the increase of Leu-M7 immunoreactivity could result from better access to the epitope when the protein is unfolded due to impaired disulfide bridge formation.

In contrast, treatment of U937 cells with the GGT inhibitor acivicin as well as treatment with other thiol effectors failed to give similar effects on anti-APN immunoreactivity. These findings strongly suggest that effects found after inhibition of PDI are not only due to the detected increase in cell surface thiols but also are directly linked to the enzymatic activity of PDI. It seems possible that PDI primarily regulates which disulfide links are formed, thus controlling the tertiary structure of APN as well as of other ectoenzymes.

Furthermore, the function of individual cysteine residues in the APN molecule for establishing correct structure and, consequently, enzymatic activity and surface expression, has not been previously studied. However, APN shares considerable sequence similarity with pyro-

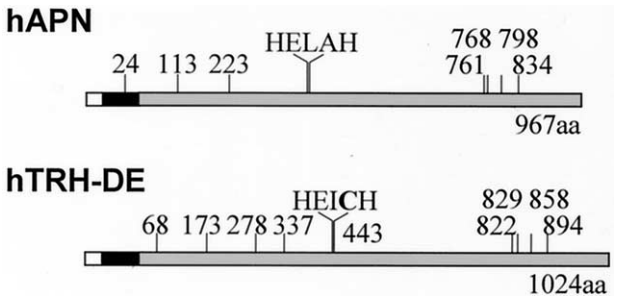

Fig. 7. Scheme of the primary structures of hAPN and hTRH-DE. The N-terminal cytoplasmic domain of both metalloproteases is given as a white box and transmembrane regions are shown as black boxes. The C-terminal extracellular domains with the indicated HEXXH motifs are represented by gray boxes. The positions of the cysteine residues are numbered and indicated by vertical lines.

glutamyl peptidase II (thyrotropin-releasing hormone degrading ectoenzyme, degrading enzyme, TRH-DE), which also belongs to the M1 family of Zn-dependent metalloproteases (Fig. 7) [43–45]. This is strikingly evident for the four cysteine residues clustered in the C-terminal region. A recent study identified TRH-DE as a disulfide-linked (via Cys68) homodimeric ectopeptidase [46]. However, covalent dimerization does not appear to be essential for its membrane expression or its enzymatic activity. Similar results were obtained in previous biochemical studies on the dimeric assembly and surface expression of APN [47]; dimerization does not seem to involve covalent bonds [38]. APN is synthesized in the RER, where it is cotranslationally inserted into the membrane and glycosylated [48,49]. It has long been assumed that high mannose content, as distinct from complex glycosylation, is required for surface expression [50,51], while dimerization is not believed to be required [47].

Both surface expression and enzymatic activity require correct folding of the extracellular domain of APN [50,52,53]. Furthermore, it was suggested that intramolecular disulfide bridges are involved in defining the tertiary structure of APN [39] and the data presented here strongly support this concept. The specific enzymatic activities of all mutants with substituted extracellular cysteine residues appeared to be significantly reduced or abolished in comparison to wild-type APN. This is in full agreement with data derived from studies concerning the cysteine substitution in TRH-DE [46]. In contrast, substituting glycine for Cys24 did not change APN enzymatic activity, indicating that, as expected, this transmembrane cysteine is not required for the formation of the correct structure of the extracellular domain of APN. As with TRH-DE, surface expression of all other cysteine mutants of APN was found to be diminished. Colocalization studies revealed intracellular retention of these mutants in the ER as shown by characteristic ER-staining patterns and a clear overlap of GFP fluorescence with an ER marker. Furthermore, treatment with Endoglycosidase H, which cleaves off the high-mannose glycans characteristic of proteins that did not reach the Golgi apparatus, confirmed this ER retardation. Taken together, these data indicate that individual cysteine residues in the extracellular part of alanyl aminopeptidase are important for tertiary structure and function of APN. However, all mutants lacking one extracellular cysteine residue could not reach the cell surface. Therefore, it was not possible to directly prove that all of these residues are critical for the surface activity once the protein has reached the cell surface. Whether the dimeric assembly of APN is also impaired by the substitution of cysteine residues remains a challenging task for future studies.

To the best of our knowledge, the data provide the first evidence of a modulation of the expression and activity of a membrane-bound exopeptidase, alanyl aminopeptidase, by oxidoreductase-mediated modulation of cell-surface thiols. It is tempting to speculate that this represents a general mechanism that could apply to other surface-bound enzymes. In support of this view, studies on thiol-disulfide interchange-mediated modulations of angiotensin-converting enzyme (ACE, CD143) on activated monocytes revealed similar results. After inhibition of PDI, the ACE enzymatic activity was diminished, whereas no quantitative changes in the surface expression of ACE molecules were observed (data not shown).

Various ectopeptidases are thought to be involved in a number of disease processes, such as inflammation and malignant transformation, which are also known to be associated with severe impairment of the thiol-disulfide status. Thus, thiol-dependent regulation of membrane-bound peptidases could be a contributing cofactor in the initiation and progression of disease. APN and other surface peptidases (e.g., dipeptidyl peptidase IV, CD26) reportedly function as regulators of leukocyte growth and function [32,54], and, therefore, inhibitors of their enzymatic activities are potent immunosuppressive, anti-inflammatory, and anti-proliferative compounds [15,55, 56]. The novel concept of a thiol-dependent regulation of surface activities introduces a new regulatory mechanism, which may contribute to the modulation of both the normal and pathological immune responses, and, consequently, to development or manifestation of autoimmune disease, allograft rejection, or malignant growth.

Acknowledgements — We are very grateful to R. H. Hädicke and A. Nehring for expert technical assistance. Furthermore, we thank Prof. Hans Sjöström for helpful comments on this manuscript. This work was supported by the Deutsche Forschungsgemeinschaft, SFB 387.

REFERENCES

[1] Rawlings, N. D.; Barrett, A. J. Evolutionary families of peptidases. *Biochem. J.* **290:**205–218; 1993.

[2] Hooper, N. M. Families of zinc metalloproteases. *FEBS Lett.* **354:**1–6; 1994.
[3] Look, A. T.; Ashmun, R. A.; Shapiro, L. H.; Peiper, S. C. Human myeloid plasma membrane glycoprotein CD13 (gp150) is identical to aminopeptidase N. *J. Clin. Invest.* **83:**1299–1307; 1989.
[4] Lerche, C.; Vogel, L. K.; Shapiro, L. H.; Noren, O.; Sjostrom, H. Human aminopeptidase N is encoded by 20 exons. *Mamm. Genome* **7:**712–713; 1996.
[5] Look, A. T.; Peiper, S. C.; Rebentisch, M. B.; Ashmun, R. A.; Roussel, M. F.; Lemons, R. S.; Le Beau, M. M.; Rubin, C. M.; Sherr, C. J. Molecular cloning, expression, and chromosomal localization of the gene encoding a human myeloid membrane antigen (gp150). *J. Clin. Invest.* **78:**914–921; 1986.
[6] Watt, V. M.; Willard, H. F. The human aminopeptidase N gene: isolation, chromosome localization, and DNA polymorphism analysis. *Hum. Genet.* **85:**651–654; 1990.
[7] Barnes, K.; Kenny, A. J.; Turner, A. J. Localization of aminopeptidase N and dipeptidyl peptidase IV in pig striatum and in neuronal and glial cell cultures. *Eur. J. Neurosci.* **6:**531–537; 1994.
[8] Noren, O.; Sjostrom, H.; Danielsen, E. M.; Cowell, G. M.; Skovbjerg, H. The enzymes of the enterocyte plasmamembrane. In: Desnuelle, P.; Sjostrom, H.; Noren, O., eds. *Molecular and cellular basis of digestion.* Amsterdam: Elsevier Science; 1986:335–365.
[9] Cohen, M. L.; Geary, L. E.; Wiley, K. S. Enkephalin degradation in the guinea-pig ileum: effect of aminopeptidase inhibitors, puromycin, and bestatin. *J. Pharmacol. Exp. Ther.* **224:**379–385; 1983.
[10] Ahmad, S.; Wang, L.; Ward, P. E. Dipeptidyl(amino)peptidase IV and aminopeptidase M metabolize circulating substance P in vivo. *J. Pharmacol. Exp. Ther.* **260:**1257–1261; 1992.
[11] Furuhashi, M.; Mizutani, S.; Kurauchi, O.; Kasugai, M.; Narita, O.; Tomoda, Y. In vitro degradation of opioid peptides by human placental aminopeptidase M. *Exp. Clin. Endocrinol.* **92:**235–237; 1988.
[12] Hoffmann, T.; Faust, J.; Neubert, K.; Ansorge, S. Dipeptidyl peptidase IV (CD 26) and aminopeptidase N (CD 13) catalyzed hydrolysis of cytokines and peptides with N-terminal cytokine sequences. *FEBS Lett.* **336:**61–64; 1993.
[13] Kanayama, N.; Kajiwara, Y.; Goto, J.; el Maradny, E.; Maehara, K.; Andou, K.; Terao, T. Inactivation of interleukin-8 by aminopeptidase N (CD13). *J. Leukoc. Biol.* **57:**129–134; 1995.
[14] Saiki, I.; Fujii, H.; Yoneda, J.; Abe, F.; Nakajima, M.; Tsuruo, T.; Azuma, I. Role of aminopeptidase N (CD13) in tumor-cell invasion and extracellular matrix degradation. *Int. J. Cancer* **54:**137–143; 1993.
[15] Pasqualini, R.; Koivunen, E.; Kain, R.; Lahdenranta, J.; Sakamoto, M.; Stryhn, A.; Ashmun, R. A.; Shapiro, L. H.; Arap, W.; Ruoslahti, E. Aminopeptidase N is a receptor for tumor-homing peptides and a target for inhibiting angiogenesis. *Cancer Res.* **60:**722–727; 2000.
[16] Larsen, S. L.; Pedersen, L. O.; Buus, S.; Stryhn, A. T cell responses affected by aminopeptidase N (CD13)-mediated trimming of major histocompatibility complex class II-bound peptides. *J. Exp. Med.* **184:**183–189; 1996.
[17] Dong, X.; An, B.; Salvucci, K. L.; Storkus, W. J.; Amoscato, A. A.; Salter, R. D. Modification of the amino terminus of a class II epitope confers resistance to degradation by CD13 on dendritic cells and enhances presentation to T cells. *J. Immunol.* **164:**129–135; 2000.
[18] Delmas, B.; Gelfi, J.; L'Haridon, R.; Vogel, L. K.; Sjostrom, H.; Noren, O.; Laude, H. Aminopeptidase N is a major receptor for the entero-pathogenic coronavirus TGEV. *Nature* **357:**417–420; 1992.
[19] Yeager, C. L.; Ashmun, R. A.; Williams, R. K.; Cardellichio, C. B.; Shapiro, L. H.; Look, A. T.; Holmes, K. V. Human aminopeptidase N is a receptor for human coronavirus 229E. *Nature* **357:**420–422; 1992.
[20] Soderberg, C.; Giugni, T. D.; Zaia, J. A.; Larsson, S.; Wahlberg, J. M.; Moller, E. CD13 (human aminopeptidase N) mediates human cytomegalovirus infection. *J. Virol.* **67:**6576–6585; 1993.
[21] Ashmun, R. A.; Look, A. T. Metalloprotease activity of CD13/aminopeptidase N on the surface of human myeloid cells. *Blood* **75:**462–469; 1990.
[22] Pinto, A.; Del Vecchio, L.; Carbone, A.; Roncadin, M.; Volpe, R.; Serraino, D.; Monfardini, S.; Colombatti, A.; Zagonel, V. Expression of myelomonocytic antigens is associated with unfavorable clinicoprognostic factors in B-cell chronic lymphocytic leukaemia. *Ann. Oncol.* **2**(Suppl. 2):107–113; 1991.
[23] Bassan, R.; Biondi, A.; Benvestito, S.; Tini, M. L.; Abbate, M.; Viero, P.; Barbui, T.; Rambaldi, A. Acute undifferentiated leukemia with CD7+ and CD13+ immunophenotype. Lack of molecular lineage commitment and association with poor prognostic features. *Cancer* **69:**396–404; 1992.
[24] Ansorge, S.; Schon, E.; Kunz, D. Membrane-bound peptidases of lymphocytes: functional implications. *Biomed. Biochim. Acta* **50:**799–807; 1991.
[25] Lendeckel, U.; Wex, T.; Ittenson, A.; Arndt, M.; Frank, K.; Mayboroda, O.; Schubert, W.; Ansorge, S. Rapid mitogen-induced aminopeptidase N surface expression in human T cells is dominated by mechanisms independent of de novo protein biosynthesis. *Immunobiology* **197:**55–69; 1997.
[26] Kunz, D.; Buhling, F.; Hutter, H. J.; Aoyagi, T.; Ansorge, S. Aminopeptidase N (CD13, EC 3.3.4.11.2) occurs on the surface of resting and concanavalin A-stimulated lymphocytes. *Biol. Chem. Hoppe Seyler* **374:**291–296; 1993.
[27] Riemann, D.; Schwachula, A.; Hentschel, M.; Langner, J. Demonstration of CD13/aminopeptidase N on synovial fluid T cells from patients with different forms of joint effusions. *Immunobiology* **187:**24–35; 1993.
[28] Riemann, D.; Wollert, H. G.; Menschikowski, J.; Mittenzwei, S.; Langner, J. Immunophenotype of lymphocytes in pericardial fluid from patients with different forms of heart disease. *Int. Arch. Allergy Immunol.* **104:**48–56; 1994.
[29] Wex, T.; Buhling, F.; Arndt, M.; Frank, K.; Ansorge, S.; Lendeckel, U. The activation-dependent induction of APN-(CD13) in T cells is controlled at different levels of gene expression. *FEBS Lett.* **412:**53–56; 1997.
[30] Lendeckel, U.; Wex, T.; Reinhold, D.; Kahne, T.; Frank, K.; Faust, J.; Neubert, K.; Ansorge, S. Induction of the membrane alanyl aminopeptidase gene and surface expression in human T cells by mitogenic activation. *Biochem. J.* **319:**817–821; 1996.
[31] Wex, T.; Lendeckel, U.; Reinhold, D.; Kahne, T.; Arndt, M.; Frank, K.; Ansorge, S. Antisense-mediated inhibition of aminopeptidase N (CD13) markedly decreases growth rates of hematopoietic tumour cells. *Adv. Exp. Med. Biol.* **421:**67–73; 1997.
[32] Lendeckel, U.; Arndt, M.; Frank, K.; Wex, T.; Ansorge, S. Role of alanyl aminopeptidase in growth and function of human T cells (review). *Int. J. Mol. Med.* **4:**17–27; 1999.
[33] Tager, M.; Kroning, H.; Thiel, U.; Ansorge, S. Membrane-bound proteindisulfide isomerase (PDI) is involved in regulation of surface expression of thiols and drug sensitivity of B-CLL cells. *Exp. Hematol.* **25:**601–607; 1997.
[34] Maellaro, E.; Dominici, S.; Del Bello, B.; Valentini, M. A.; Pieri, L.; Perego, P.; Supino, R.; Zunino, F.; Lorenzini, E.; Paolicchi, A.; Comporti, M.; Pompella, A. Membrane γ-glutamyl transpeptidase activity of melanoma cells: effects on cellular H(2)O(2) production, cell surface protein thiol oxidation, and NF-κB activation status. *J. Cell Sci.* **113:**2671–2678; 2000.
[35] Olsen, J.; Cowell, G. M.; Konigshofer, E.; Danielsen, E. M.; Moller, J.; Laustsen, L.; Hansen, O. C.; Welinder, K. G.; Engberg, J.; Hunziker, W. Complete amino acid sequence of human intestinal aminopeptidase N as deduced from cloned cDNA. *FEBS Lett.* **238:**307–314; 1988.
[36] Olsen, J. Molecular biology of aminopeptidase N: amino acid sequence, gene structure, and tissue-specific gene regulation. Dissertation, Landskrona, Sweden, 1998.
[37] Hussain, M. M. Reconstitution of purified dipeptidyl peptidase IV. A comparison with aminopeptidase N with respect to mor-

phology and influence of anchoring peptide on function. *Biochim. Biophys. Acta* **815:**306–312; 1985.
[38] Sjostrom, H.; Noren, O. Changes of the quaternary structure of microvillus aminopeptidase in the membrane. *Eur. J. Biochem.* **122:**245–250; 1982.
[39] Sjostrom, H.; Noren, O.; Olsen, J. Structure and function of aminopeptidase N. *Adv. Exp. Med. Biol.* **477:**25–34; 2000.
[40] Lendeckel, U.; Wex, T.; Kahne, T.; Frank, K.; Reinhold, D.; Ansorge, S. Expression of the aminopeptidase N (CD13) gene in the human T cell lines HuT78 and H9. *Cell Immunol.* **153:**214–226; 1994.
[41] Freedman, R. B.; Hawkins, H. C.; McLaughlin, S. H. Protein disulfide-isomerase. *Methods Enzymol.* **251:**397–406; 1995.
[42] Ashmun, R. A.; Shapiro, L. H.; Look, A. T. Deletion of the zinc-binding motif of CD13/aminopeptidase N molecules results in loss of epitopes that mediate binding of inhibitory antibodies. *Blood* **79:**3344–3349; 1992.
[43] Bauer, K. Purification and characterization of the thyrotropin-releasing hormone-degrading ectoenzyme. *Eur. J. Biochem.* **224:** 387–396; 1994.
[44] Schauder, B.; Schomburg, L.; Kohrle, J.; Bauer, K. Cloning of a cDNA encoding an ectoenzyme that degrades thyrotropin-releasing hormone. *Proc. Natl. Acad. Sci. USA* **91:**9534–9538; 1994.
[45] Schomburg, L.; Turwitt, S.; Prescher, G.; Lohmann, D.; Horsthemke, B.; Bauer, K. Human TRH-degrading ectoenzyme cDNA cloning, functional expression, genomic structure, and chromosomal assignment. *Eur. J. Biochem.* **265:**415–422; 1999.
[46] Papadopoulos, T.; Heuer, H.; Bauer, K. Analysis of the thyrotropin-releasing hormone-degrading ectoenzyme by site-directed mutagenesis of cysteine residues Cys68 is involved in disulfide-linked dimerization. *Eur. J. Biochem.* **267:**2617–2623; 2000.
[47] Danielsen, E. M. Dimeric assembly of enterocyte brush border enzymes. *Biochemistry* **33:**1599–1605; 1994.
[48] Danielsen, E. M.; Noren, O.; Sjostrom, H. Co- and post-translational events in the biogenesis of pig small intestinal aminopeptidase N. *Tokai. J. Exp. Clin. Med.* **7**(Suppl.):135–140; 1982.
[49] Danielsen, E. M.; Noren, O.; Sjostrom, H. Biosynthesis of intestinal microvillar proteins. Processing of aminopeptidase N by microsomal membranes. *Biochem. J.* **212:**161–165; 1983.
[50] Danielsen, E. M.; Cowell, G. M. Biosynthesis of intestinal microvillar proteins. Further characterization of the intracellular processing and transport. *FEBS Lett.* **166:**28–32; 1984.
[51] Danielsen, E. M.; Cowell, G. M.; Noren, O.; Sjostrom, H.; Dorling, P. R. Biosynthesis of intestinal microvillar proteins. The effect of swainsonine on post-translational processing of aminopeptidase N. *Biochem. J.* **216:**325–331; 1983.
[52] Danielsen, E. M. Folding of intestinal brush border enzymes. Evidence that high-mannose glycosylation is an essential early event. *Biochemistry* **31:**2266–2272; 1992.
[53] Danielsen, E. M. Post-translational suppression of expression of intestinal brush border enzymes by fructose. *J. Biol. Chem.* **264:** 13726–13729; 1989.
[54] Kahne, T.; Lendeckel, U.; Wrenger, S.; Neubert, K.; Ansorge, S.; Reinhold, D. Dipeptidyl peptidase IV: a cell surface peptidase involved in regulating T cell growth (review). *Int. J. Mol. Med.* **4:**3–15; 1999.
[55] Reinhold, D.; Hemmer, B.; Gran, B.; Steinbrecher, A.; Brocke, S.; Kahne, T.; Wrenger, S.; Born, I.; Faust, J.; Neubert, K.; Martin, R.; Ansorge, S. Dipeptidyl peptidase IV (CD26): role in T cell activation and autoimmune disease. *Adv. Exp. Med. Biol.* **477:** 155–160; 2000.
[56] Pauly, R. P.; Demuth, H. U.; Rosche, F.; Schmidt, J.; White, H. A.; Lynn, F.; McIntosh, C. H.; Pederson, R. A. Improved glucose tolerance in rats treated with the dipeptidyl peptidase IV (CD26) inhibitor Ile-thiazolidide. *Metabolism* **48:**385–389; 1999.

ABBREVIATIONS

Ala-pNA—alanylparanitroanilide
APN—aminopeptidase N
B-ALL—acute B cell leukemia
BSA—bovine serum albumin
BSO—buthionine sulfoximine
CD—cluster of differentiation
CML—chronic myeloid leukemia
CMV—cytomegalovirus
ER—endoplasmic reticulum
FACS—fluorescence-activated cell sorting
FCS—fetal calf serum
GFP—green fluorescent protein
HRP—horseradish peroxidase
mfi—mean fluorescence intensity
NEM—N-ethylmaleimide
NHL—non-Hodgkin lymphoma
PAGE—polyacrylamide gel electrophoresis
PBS—phosphate-buffered saline
PE—phycoerythrin
PNGase F—peptide N-glycosidase F
SDS—sodiumdodecylsulfate
TRH-DE—thyrotropin-releasing hormone-degrading ectoenzyme